Coincidence of the Molecular Organization of β-Substituted Oligothiophenes in Two-Dimensional Layers and Three-Dimensional Crystals

Reiko Azumi,[b] Günther Götz,[a] Tony Debaerdemaeker,[c] and Peter Bäuerle*[a]

Dedicated to Prof. Dr. Dr. Franz Effenberger on the occasion of his 70th birthday

Abstract: The molecular arrangements of three different alkyl-substituted oligothiophenes both in two-dimensional adsorbed layers at a substrate interface and in bulk three-dimensional crystals were studied. Scanning tunneling microscopy (STM) was used to investigate the ordering of the conjugated oligomers in two-dimensional layers adsorbed on graphite. These data were compared with the X-ray structure determinations of single crystals revealing the arrangement in the three-dimensional bulk material. Quaterthiophenes **1** and **2**, bearing dodecyl and hexyl side chains, respectively, exhibit a lamella-type stacking of the conjugated backbone concomitant with an interlocking of the alkyl side chains both on the surface and in the crystal. In contrast, the arrangement of propyl-substituted quaterthiophene **3** is rather "herringbone-like" due to the reduced interactions of the shorter alkyl side chains. In all three cases, evidently, the two-dimensional ordering at the graphite surface is coincident with the molecular packing in one cross-section of the three-dimensional crystal.

Keywords: monolayers · oligothiophenes · scanning tunneling microscopy · self-assembly · structure elucidation

Introduction

Polythiophenes[1] and corresponding oligomers[2] have been intensively studied as promising materials for electronic devices.[3] Excellent electronic and transport properties combined with good stability under ambient conditions allow their application in, for example, organic light emitting diodes[4] or thin-film transistors.[5] Many investigations on polythiophenes therefore have been devoted to the understanding how structural parameters affect the physical properties.[6] Since in most applications these materials are used in the solid state much interest has also been focussed on the molecular packing of the polymers in the bulk. Mainly X-ray diffraction measurements on the partly crystalline polymers give valuable hints about the three-dimensional structure, which definitely affects the physical properties.[7] More ordered materials give rise to better performances of the electronic devices. Excellent examples are regioregularly head-to-tail coupled poly(3-alkylthiophene)s often exhibiting superior properties than the corresponding regiorandom derivatives.[8] The mean conjugation length in solution and the tendency to order in the solid state increases with increasing regioregularity. Therefore, much interest has been focussed on the understanding of the detailed molecular packing of the bulk compounds.[9]

Since these conjugated polymers are polydisperse, the characterization of α-conjugated oligothiophenes with a well-defined chemical structure and chain length is of great importance in order to elucidate structure – property relationships. Additionally, it has been well demonstrated that oligothiophenes themselves represent excellent candidates for electronic materials. With respect to structure determinations in the solid state, however, due to their highly anisotropic shape and the resulting difficulties to crystallize these compounds, X-ray structure determinations on oligothiophenes become only recently more and more prominent.[6, 10]

Scanning tunneling microscopy (STM) offers an alternative way to investigate molecular arrangements of organic compounds. It has been found that alkylcyanobiphenyls,[11] *n*-alkanes,[12] cycloalkanes,[13] fatty acids,[12b, 14] alkylbenzenes,[12b] and more complicated molecules, mostly with planar and extended π-systems,[15] all bearing longer alkyl chains are adsorbed from a solution or a melt to the surface of highly oriented pyrolytic graphite (HOPG) or molybdenum disulfide

[a] Prof. Dr. P. Bäuerle, Dr. G. Götz
Abteilung Organische Chemie II der Universität Ulm
Albert-Einstein-Allee 11, 89081 Ulm (Germany)
Fax: (+49) 731-502-2840
E-mail: peter.baeuerle@chemie.uni-ulm.de

[b] Dr. R. Azumi
National Institute of Materials and Chemical Research
Tsukuba, Ibaraki 305-8565 (Japan)

[c] Prof. Dr. T. Debaerdemaeker
Sektion Röntgen- und Elektronenbeugung der Universität Ulm
Albert-Einstein-Allee 11, 89081 Ulm (Germany)

  0947-6539/00/0604-0735 $ 17.50+.50/0

(MoS_2) and form ordered monolayers. Frequently, the alkyl chains align along one of the main crystallographic axes of the substrate. Additionally, STM also provides information about intermolecular and interfacial interactions, which are important from the viewpoint of applying these materials in thin-film devices. Another advantage of the STM technique is that the local ordering, such as dynamic processes of domain boundaries or the existence and size of defects, can be studied. Besides the investigation of monolayers at the solid–liquid interface and apart from a tremendous amount of work on vacuum-evaporated films,[16] several studies on cast films have revealed ordering and commensurability of the molecules with the underlying substrate.[17] Vacuum sublimation and casting of films may then allow the investigation of molecules that can not be physisorbed from solution due to the lack of suited substituents.

We and others have reported that several alkylated oligothiophenes form ordered monolayers at the solid–liquid interface.[18] It seems to be a general rule that oligomers with alkyl substituents at β-positions tend to self-assemble on HOPG. The ease of formation of the physisorbed monolayer strongly depends on the structure and the length of the oligothiophene, which determines the adsorption–desorption equilibrium. In contrast, α- and α,α'-substituted derivatives are rarely adsorbed on HOPG but preferably on MoS_2.[18f]

The molecular arrangements in the physisorbed monolayers determined with the STM technique may give valuable hints for the discussion of the properties of the bulk material. It is, however, not easy to determine from STM pictures if a particular molecular order is rather due to molecule–molecule interactions or dominated by epitaxial effects owing to the substrate surface. Therefore, it would be highly desirable and extremely useful if one could deduce from two-dimensional arrangements information about three-dimensional packing motifs. Herein for the first time, we demonstrate that in each case of three differently substituted oligothiophenes **1**–**3**, the molecular organization in the two-dimensional self-assembled monolayer fully coincides with the packing in one cross-section of the three-dimensional crystal.

Abstract in Japanese:

異なる長さのアルキル側鎖をもつ３種類のチオフェン４量体の、２次元吸着膜内および単結晶内での分子配列について検討した。グラファイト基板上に吸着した単分子膜内でのオリゴチオフェン分子の配列をＳＴＭを用いて観察し、Ｘ線単結晶構造解析から得られた３次元の結晶内での配列との比較を試みた。アルキル側鎖の長い（dodecyl および hexyl）誘導体の吸着単分子膜では、アルキル基同士が interdigitate し共役主鎖部分が互いに平行にスタックしたラメラ状の配列がみられた。一方、アルキル側鎖の短い（propyl）誘導体では herringbone タイプの配列となった。いずれの場合にも、グラファイト上の吸着単分子膜内での分子配列は、３次元結晶内のある「断面」での分子配列にきわめて類似していることが明らかになった。

Abstract in German: *Das Selbstorganisationsverhalten von drei unterschiedlich alkylsubstituierten Oligothiophenen wird sowohl in zweidimensionalen Monoschichten, die an einer Substrat-Grenzfläche adsorbiert sind, als auch in dreidimensionalen Kristallen untersucht. Rastertunnelmikroskopie (STM) wurde als Methode verwendet, um die Selbstorganisation der konjugierten Oligomeren in adsorbierten zwei-dimensionalen Schichten zu untersuchen. Diese Daten werden dann mit denen von Röntgenstrukturanalysen verglichen, die Aufschluß über die molekulare Ordnung im drei-dimensionalen Festkörper geben. Die Quaterthiophene **1** und **2**, die Dodecyl- bzw. Hexylseitenketten tragen, zeigen eine lamellenartige Anordnung der konjugierten Moleküle, die das Ineinandergreifen der Alkylketten benachbarter Moleküle sowohl auf der Oberfläche als auch im Kristall beinhalten. Im Gegensatz dazu ist die Anordnung des propylsubstituierten Quaterthiophenes **3** wegen der verminderten Wechselwirkungen der kürzeren Alkylketten eher "fischgrätenartig". Überraschenderweise stimmt in allen drei Fällen die Anordnung der Moleküle in der zwei-dimensionalen Monoschicht auf Graphit mit der in einer Ebene im drei-dimensionalen Kristall überein.*

Results

Syntheses: The 3,3‴-dialkylated quaterthiophenes **1**,[18b] **2**, and **3** have been effectively prepared by the nickel-catalyzed cross-coupling of the Grignard reagent of 3-dodecyl-2-bromothiopene, 3-hexyl-2-bromothiopene, and 3-propyl-2-bromothiophene with 5,5′-dibromo-2,2′-bithiophene (44–88%) (Scheme 1).

Single crystals suited for X-ray structure analyses were grown by slow evaporation of quaterthiophene **1** from *n*-hexane, **2** from *n*-hexane/ethanol, and **3** from petroleum ether.

STM investigations on the adsorbed two-dimensional layers: Dodecyl-substituted oligothiophene **1** is adsorbed at the solution–HOPG interface and forms a stable monolayer. The molecular image usually appears immediately after bringing the solution of the oligomer in 1,2,4-trichlorobenzene onto the (001) face of HOPG. A large scale STM image reveals good ordering (Figure 1). Domains with various size from several tens to several hundreds of nanometers are formed. In the domains the individual oligomers are perfectly arranged in a lamella-type orientation forming bright rows which are separated by about 2 nm from the adjacent ones. The rows are aligned in only six different directions, which suggests that the orientation of the molecules is affected by the HOPG substrate, which bears three-fold axes.[15g] A dynamic change of the domain boundaries with time is observed, as was also reported for adsorbed monolayers of octadecanol[12b] or alkylated octithiophene and anthraquinone molecules.[15a]

Figure 2 (right) shows an image of a smaller area with molecular resolution. It provides a closer look into a well-ordered domain. Each molecule in the bright rows is clearly seen, and in analogy to previous results we correlate the brighter spots to the oligothiophene backbone.[15a, 18] The alkyl chains are supposed to lie between the brighter spots. A similar molecular arrangment was observed for a dip-coated film of **1** from a chloroform solution onto HOPG (data not shown). The model of the molecular arrangement (Figure 2

0947-6539/00/0604-0736 $ 17.50+.50/0 *Chem. Eur. J.* **2000**, *6*, No. 4

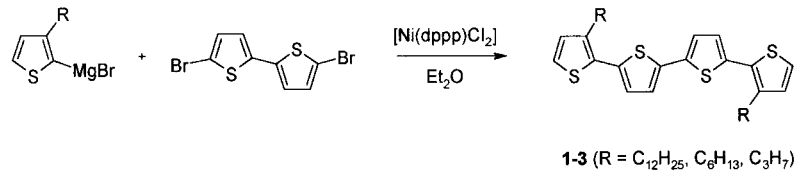

1-3 (R = $C_{12}H_{25}$, C_6H_{13}, C_3H_7)

Scheme 1. Synthesis of oligothiophenes **1**–**3** by nickel-catalyzed cross-coupling.

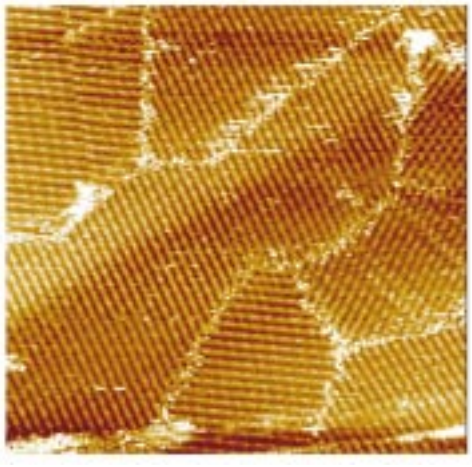

Figure 1. STM height image (100×100 nm^2) of quaterthiophene **1** adsorbed on HOPG (bias voltage: 700 mV, sample is positive, tunnel current: 40.5 pA).

left) supports that the molecules cover the surface as densely as possible. The lattice constants of the two-dimensional layer were determined to be $A = 1.23 \pm 0.10$ nm, $B = 2.15 \pm 0.05$ nm, $\Gamma = 75° \pm 3°$ (Table 1). The underlying graphite lattice (Figure 2, right, inset) was observed by decreasing the voltage after the molecular image had been taken. One of the main crystallographic axes of HOPG has an angle of $85° \pm 3°$ with respect to the oligothiophene backbone. If the long axis of the alkyl chains is assumed to be oriented perpendicularly with respect to the oligothiophene backbone, as it is drawn in Figure 2, then the alkyl chains align along the main crystallographic axis of the substrate. This was also found for adsorbed monolayers of other compounds.[12–15] This finding will be discussed later again.

Table 1. Unit-cell parameters of the two-dimensional adsorbates at HOPG compared with the "sheets" in the three-dimensional single crystals.

Oligo-thiophene	two-dimensional adsorbate on HOPG	"cross-section" of the three-dimensional crystal
1	$A = 1.23 \pm 0.10$ nm	$A = 1.23$ nm
	$B = 2.15 \pm 0.05$ nm	$B = 2.14$ nm
	$\Gamma = 75 \pm 3°$	$\Gamma = 75.4°$
2	$A = 1.21 \pm 0.05$ nm	$A = 1.22$ nm
	$B = 1.46 \pm 0.05$ nm	$B = 1.50$ nm
	$\Gamma = 81 \pm 3°$	$\Gamma = 81.7°$
3	$A = 1.65 \pm 0.10$ nm	$A = 1.59$ nm
	$B = 1.70 \pm 0.20$ nm	$B = 1.49$ nm
	$\Gamma = 87 \pm 4°$	$\Gamma = 84.9°$

The orientation and packing of hexyl-substituted quaterthiophene **2** at the solution–substrate interface are similar to that of **1**, except that the distance between the adjacent rows (ca. 1.5 nm) is smaller than that for **1** (ca. 2 nm) due to the shorter alkyl side chains (Figure 3, right). This result shows that a *n*-hexyl side chain is evidently still sufficiently long to form and stabilize self-assembled monolayers at the substrate surface. The lattice constants of the two-dimensional layer were similar to those of oligomer **1**, except for *B*, which is shorter and represents the separation between the rows (Table 1). The model of the molecular arrangement of oligomer **2** is illustrated in Figure 3 (left).

However, a monolayer of *n*-propyl-substituted quaterthiophene **3** was not observed at the solution–HOPG interface. Clearly, owing to the shorter side chains the molecules can not provide sufficient interactions to the substrate surface. Instead, self-assembled monolayers were successfully observed for dip-coated films from a chloroform solution, as shown in Figure 4 (right). The molecular arrangment of oligomer **3** is obviously quite different from those of derivatives **1** and **2**, suggesting that the *n*-propyl group is too short to stack with one another in order to form the parallel lamella-type arrangement as the other two derivatives do. The nearest neighboring molecules are not parallel with each other and form a "herringbone-like" structure, in which each molecule is nearly perpendicular to the surrounding ones. The lattice constants of the two-dimensional layer were therefore different from the other oligomers (Table 1). The model of the molecular arrangement of oligomer **3** is illustrated in Figure 4 (left).

X-ray single-crystal analyses

Molecular parameters: Crystals of quaterthiophene **1** are blade-like and grow very often into twins. Figure 5 shows the crystal structure of **1**. Structural features, experimental conditions and crystal data are collected in Tables 2 and 3. The quaterthiophene moiety has an all-*anti* structure with a dihedral angle of 12.2° between the outer thiophene ring and the inner one. The alkyl side chains exhibit an all-*trans* conformation and are positioned nearly perpendicularly with respect to the oligothiophene backbone. Furthermore, the thiophene rings and the carbon skeleton of the alkyl side chains are nearly coplanar (Figure 5).

Compound **2** also crystallizes in a blade-like shape from *n*-hexane/ethanol. When the crystallization is attempted at room temperature, the oligothiophene precipitates as an oil because of its very low melting point. The crystallization was therefore performed at 4 °C. The low melting point proves that the intermolecular forces of this compound are relatively weak. Similar to dodecylquaterthiophene **1**, hexyl-substituted derivative **2** in the crystal adopts a nearly planar all-*anti* conformation with a dihedral angle of 10.2° between the outer and the inner thiophene rings (Figure 6). The alkyl side chains adopt an all-*trans* arrangement and are nearly perpendicularly extended to the oligothiophene backbone.

Dipropyl derivative **3** crystallized as platelets. Two independent molecules, which are oblique to each other, exist in the unit cell (Figure 7). The oligothiophene moiety maintains an all-*anti* conformation; however, a larger twist exists between adjacent thiophene rings (19.2° for molecule a and 14.6° for molecule b in the unit cell) in comparison with the twists found for compounds **1** and **2**. The propyl side chain of molecule b unfortunately displays certain disorder so that the position of carbons could not be properly refined.

We note a common tendency for all three compounds, that the C–C and C–S bond lengths at the edge of the molecule are slightly shorter (see Table 2: e.g., for **1**: C1–C2 1.34 Å vs. C5–C6 1.36 Å; C1–S1 1.70 Å vs. S2–C5 1.73 Å) in comparison with the other corresponding bonds. This phenomenon is also observed in X-ray structure determinations of other oligothiophenes.[10c–e,n,o] This finding is likely due to the electronic nature of conjugated backbone and is in accordance with semiempirical and ab initio calculations on individual molecules excluding intermolecular interactions.[19]

However, some uncertainty in the X-ray analysis due to rotational oscillations[20] of the corresponding atoms can not be totally excluded at the moment. Another general feature is the larger twist between the outer and the inner thiophene rings compared with unsubstituted oligothiophenes. This has been observed as well for other β-substituted oligothiophenes[10i,n,o] and is due to the steric hindrance of the α-methylene group in the alkyl side chain and the sulfur atom (S2) on the adjacent thiophene ring. This is reflected in the distance between C9 and S2, which is, for example, 3.18 Å for compound **1** and is much smaller than the

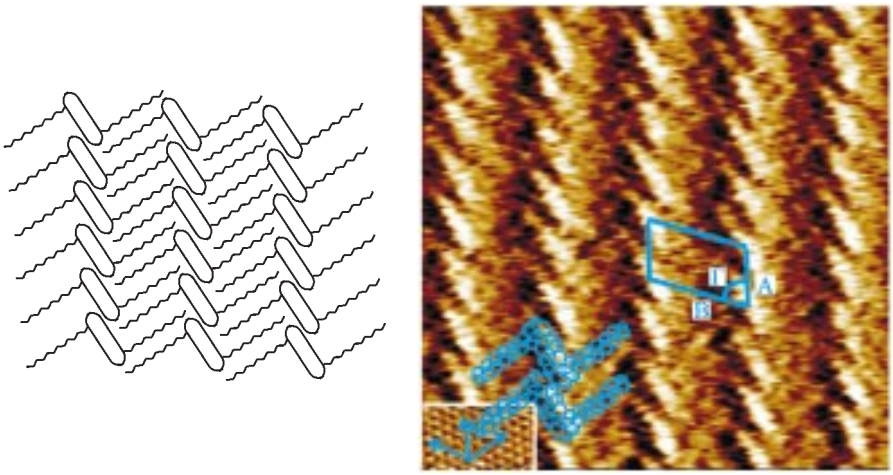

Figure 2. Right: STM current image of a small area (10×10 nm^2) of quaterthiophene **1** adsorbed on HOPG (bias voltage: 500 mV, sample is positive, tunnel current: 48 pA). The inset shows the underlying HOPG substrate (bias voltage: 20 mV, sample is positive, tunnel current: 50 pA). Left: model of the molecular arrangement.

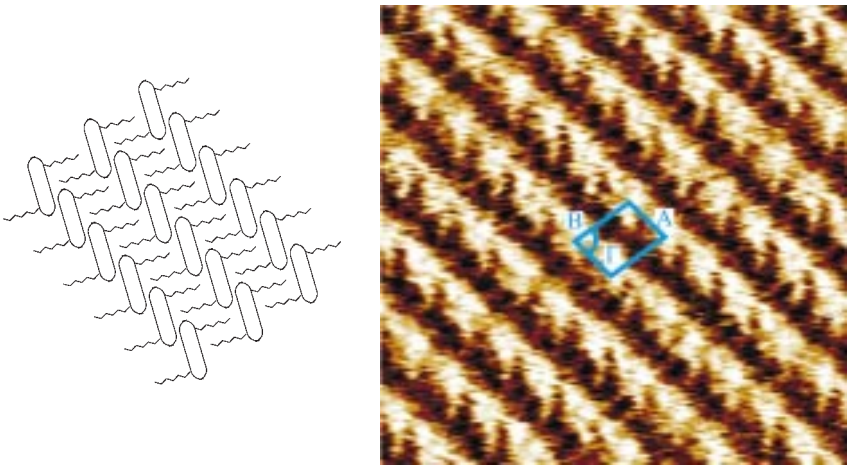

Figure 3. Right: STM current image (10×10 nm^2) of quaterthiophene **2** adsorbed on HOPG (bias voltage: 350 mV, sample is positive, tunnel current: 35 pA). Left: model of the molecular arrangement.

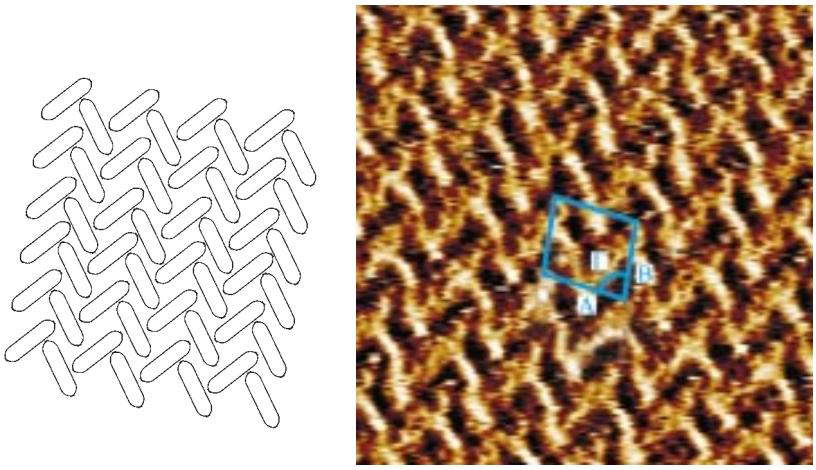

Figure 4. Right: STM current image (10×10 nm^2) of quaterthiophene **3** dip-coated on HOPG from a chloroform solution (bias voltage: -540 mV, sample is negative, tunnel current: 20 pA). Left: model of the molecular arrangement. Alkyl chains are not drawn since it is ambiguous from STM pictures if the molecules are "in-plane" or not.

0947-6539/00/0604-0738 $ 17.50+.50/0 *Chem. Eur. J.* **2000**, *6*, No. 4

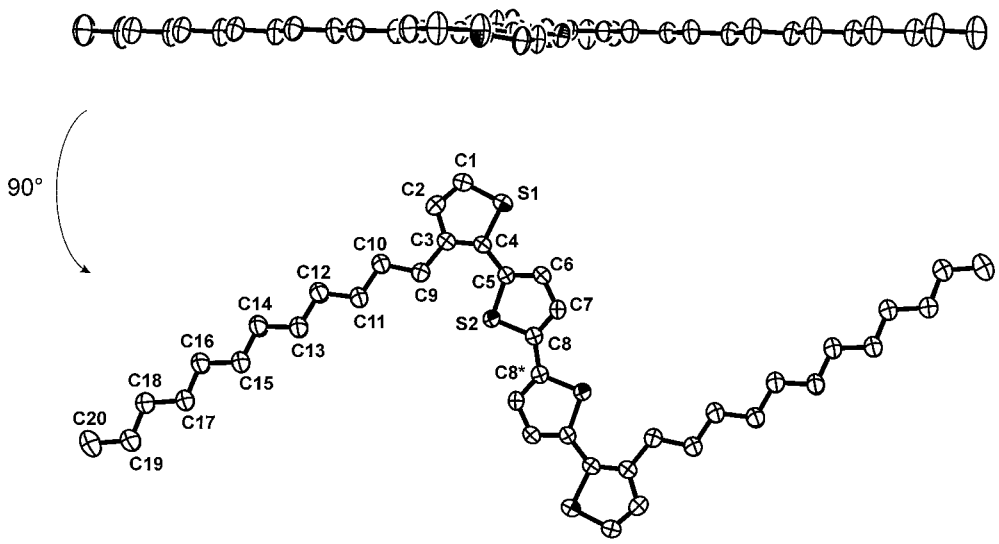

Figure 5. Molecular structure of quaterthiophene **1** with the atomic numbering scheme. Displacement ellipsoids are drawn at the 50% probability level.

Table 2. Selected structural features of **1**–**3**.[a]

	1	**2**	**3a**	**3b**
bond lengths [Å]				
S(1)-C(1)	1.698(3)	1.714(5)	1.694(5)	1.721(8)
S(1)-C(4)	1.740(3)	1.732(4)	1.729(4)	1.704(6)
S(2)-C(5)	1.733(2)	1.741(4)	1.734(4)	1.729(5)
S(2)-C(8)	1.726(3)	1.731(4)	1.721(4)	1.722(5)
C(2)-C(1)	1.338(3)	1.351(6)	1.333(6)	1.360(6)
C(2)-C(3)	1.416(3)	1.425(6)	1.424(6)	1.417(9)
C(3)-C(9)	1.519(3)	1.497(6)	1.492(6)	1.491(13)
C(4)-C(3)	1.366(4)	1.378(6)	1.362(6)	1.337(8)
C(5)-C(4)	1.457(3)	1.460(6)	1.460(6)	1.457(7)
C(5)-C(6)	1.359(4)	1.355(6)	1.347(6)	1.353(7)
C(7)-C(6)	1.405(3)	1.403(7)	1.410(5)	1.394(7)
C(8)-C(7)	1.355(3)	1.368(6)	1.361(5)	1.287(9)
C(8)-C(8)[b–e]	1.454(5)[b]	1.467(8)[c]	1.454(7)[d]	1.443(9)[e]
bond angles [°]				
C(1)-C(2)-C(3)	113.8(2)	114.7(4)	113.8(5)	113.4(5)
C(1)-S(1)-C(4)	91.8(1)	92.0(2)	91.7(3)	91.5(4)
C(2)-C(1)-S(1)	112.0(2)	111.0(3)	112.1(4)	111.1(6)
C(3)-C(4)-C(5)	133.0(2)	130.9(4)	131.9(4)	131.6(6)
C(3)-C(4)-S(1)	110.4(2)	111.5(3)	111.1(3)	110.8(5)
C(4)-C(3)-C(2)	112.0(2)	110.8(4)	111.3(4)	112.1(7)
C(5)-C(6)-C(7)	114.1(2)	115.1(4)	114.7(4)	114.9(5)
C(6)-C(5)-C(4)	127.8(2)	127.8(4)	127.7(4)	127.5(5)
C(6)-C(5)-S(2)	109.3(2)	109.3(3)	109.4(3)	108.9(4)
C(7)-C(8)-C(8)[b–e]	129.5(3)[b]	130.1(5)[c]	129.2(5)[d]	129.3(6)[e]
C(7)-C(8)-S(2)	110.0(2)	110.4(3)	110.3(3)	109.7(4)
C(8)-C(7)-C(6)	113.8(3)	112.7(4)	112.8(4)	113.4(5)
C(8)-S(2)-C(5)	92.9(1)	92.5(2)	92.8(2)	93.1(3)

[a] Numbering as defined in X-ray analyses (see figures 5–7). [b] Symmetry transformations used to generate equivalent atoms: $-x, -y, -z$. [c] Symmetry transformations used to generate equivalent atoms: $-x, -y+1, -z+2$. [d] Symmetry transformations used to generate equivalent atoms: $-x+1, -y+1, -z+1$. [e] Symmetry transformations used to generate equivalent atoms: $-x-1, -y+2, -z$.

Table 3. Structure determination summary of **1**–**3**.

	1	**2**	**3**
formula	$C_{40}H_{58}S_4$	$C_{28}H_{34}S_4$	$C_{22}H_{22}S_4$
M_w	667.10	498.79	414.64
T [K]	293(2)	220(2)	293(2)
crystal system	triclinic	triclinic	triclinic
space group	$P\bar{1}$	$P\bar{1}$	$P\bar{1}$
a [Å]	5.581(1)	6.854(1)	5.503(1)
b [Å]	12.268(2)	9.441(1)	13.267(2)
c [Å]	14.428(3)	10.854(1)	14.922(2)
α [°]	98.92(2)	106.59(2)	77.11(2)
β [°]	93.77(2)	92.85(2)	81.99(2)
γ [°]	100.83(2)	101.61(2)	81.26(2)
V [Å^3]	953.9(3)	655.1(2)	1043.3(3)
Z	1	1	2
ρ_{calcd} [Mg m^{-3}]	1.161	1.264	1.320
μ [mm^{-1}]	0.275	0.377	0.459
$F(000)$	362	266	436
crystal size [mm]	0.06 × 0.27 × 0.65	0.15 × 0.50 × 0.23	0.06 × 0.23 × 0.46
color	orange	yellow	yellow
scan range (θ) [°]	3.08–25.97	2.31–25.91	2.82–24.10
index ranges	$-6 \le h \le 6$	$-8 \le h \le 8$	$-6 \le h \le 5$
	$-15 \le k \le 14$	$-11 \le k \le 11$	$-15 \le k \le 15$
	$-17 \le l \le 17$	$-13 \le l \le 13$	$-17 \le l \le 17$
reflections collected/unique	8217/3456	5640/2377	7405/3104
R(int)	0.0713	0.0587	0.0583
data/restraints/parameters	3456/0/199	2377/0/145	3104/0/235
goodness-of-fit on F^2	0.709	1.106	0.816
final R indices [$I > 2\sigma(I)$] $R1$	0.0422	0.0615	0.0482
$wR2$	0.0627	0.1927	0.1148
R indices (all data) $R1$	0.1270	0.0872	0.1122
$wR2$	0.0749	0.2007	0.1302
largest diff. peak/hole [e Å^{-3}]	0.184/−0.159	0.852/−0.334	0.458/−0.451

sum of van der Waals radii of carbon (1.7 Å) and sulfur (1.8 Å).[21]

Crystal packing: Dodecylquaterthiophene **1** exhibits a quite unique molecular packing in the bulk crystal. The conjugated backbones of the molecules are coplanar and form a layered structure that consists of slipped stacks as is seen in the view from the [010] direction (Figure 8, top). The interlayer distance is 3.41 Å, indicating that the molecules are rather tightly packed. The quaterthiophene backbones of adjacent molecules in the stack are laterally displaced and only slightly overlap (closest C–C distance in accordance with the layer-to-layer distance: 3.45 Å; closest S–S distance: 3.71 Å). None of the distances between intermolecular non-hydrogen atoms are shorter than the sum of the van der Waals radii; this indicates that there is no unusual intermolecular interaction.

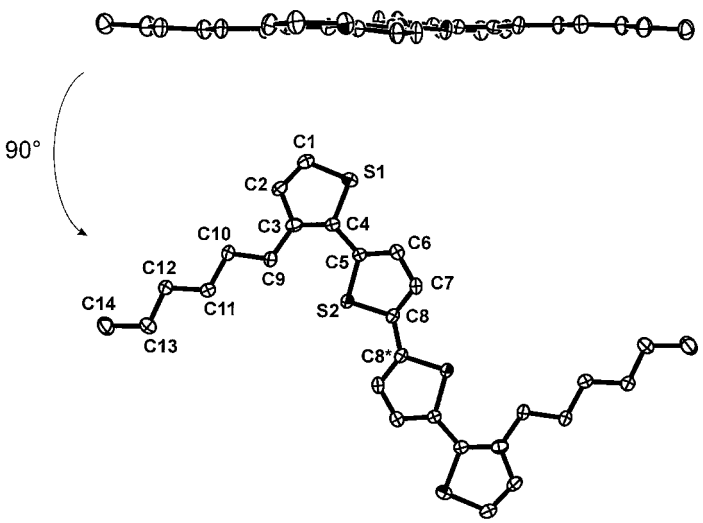

Figure 6. Molecular structure of quaterthiophene **2** with the atomic numbering scheme. Displacement ellipsoids are drawn at the 50% probability level.

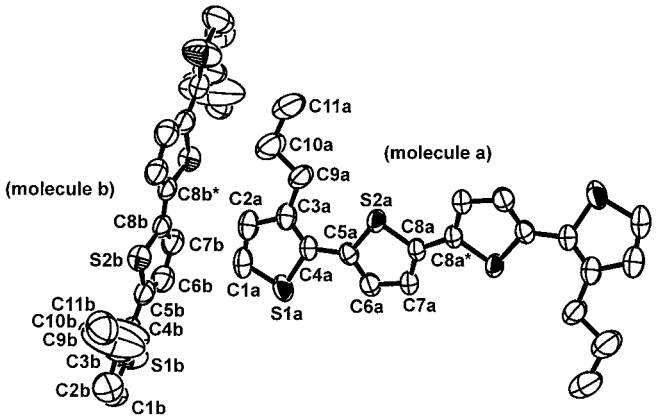

Figure 7. Molecular structure of quaterthiophene **3** with the atomic numbering scheme. Displacement ellipsoids are drawn at the 50% probability level.

This packing motif is in striking contrast to the usually observed "herringbone" arrangement in oligothiophene structure determinations.[10] Oligothiophene **1** indeed represents one of the very few examples of crystal structures in which all the planes of the oligothiophene backbones are parallel to one another.[10q] This ordering may arise from the bulky long alkyl side chains stretched almost perpendicularly with respect to the π-system and preventing the "herringbone" arrangement. The crystal structure of compound **1** therefore is an excellent model for poly(alkylthiophene)s,[3] which are also believed to exhibit a face-to-face π-stacking.

In the (103) plane, all molecules lie flat and form a lamella-type structure that contains rows of the oligothiophenes which are separated by approximately 20 Å (Figure 8, bottom). The alkyl side chains of adjacent rows interlock providing optimal van der Waals interactions. The planar molecules thus form a two-dimensional "sheet", which is identical to the (103) plane.

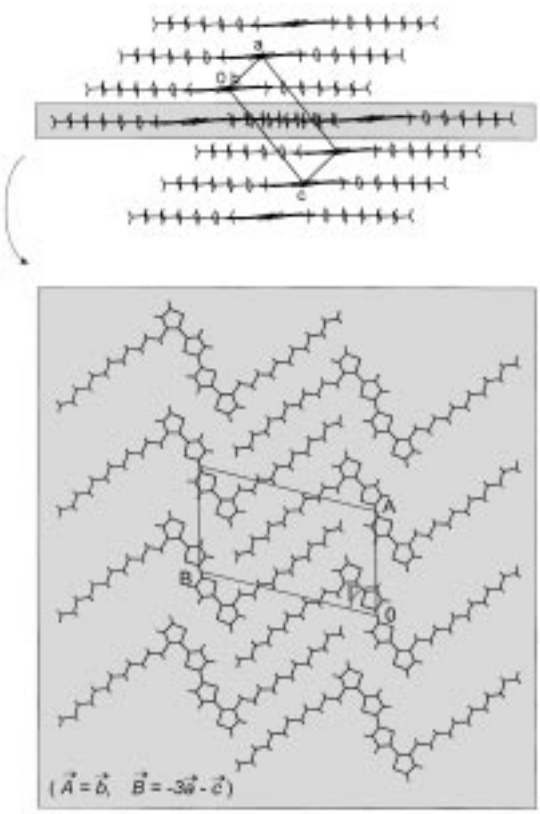

Figure 8. Molecular packing of **1** viewed from the [010] direction (top). View from the direction normal to the (103) plane (bottom). Only the molecules on the same plane are drawn. The correlation of the two-dimensional and the three-dimensional lattices is given at the bottom of the figure.

The molecular arrangement observed in this plane of the bulk crystal of **1** (Figure 8, bottom) has an intriguing coincidence with the arrangement of the molecules in the two-dimensional monolayers at the solution–HOPG interface (Figure 2). The "lattice constants" in the "sheet" in the three-dimensional crystal and those observed in the two-dimensional monolayer are almost identical (Table 1); this suggests that the molecular arrangement in the two-dimensional layer at the HOPG surface is identical with one layer in the bulk crystal.

The molecular packing of hexyl-substituted derivative **2** in the crystal is similar to that of oligothiophene **1**. Viewed from the [011] direction, we find again a layered structure that consists of slipped π-stacks of coplanar conjugated backbones. The resulting interlayer distance is 3.62 Å and is larger than that of compound **1** (Figure 9, top). Viewed from the direction normal to the (1 −22) plane, the same arrangement of the quaterthiophene units in parallel lamellae is evident, and "sheets" that contain interlocking alkyl side chains are formed (Figure 9, bottom). However, in this case the overlap of π-conjugated systems between the neighboring "sheets" is smaller than in **1**, and the slipping is increased: the shortest intermolecular distance between atoms in the oligothiophene backbones increases to 3.70 Å. Due to the shorter chain length, on the other hand, the separation between the rows is decreased to about 1.5 nm. Also in the case of the hexyl-substituted derivative **2** the packing motif in the (1 −22)

0947-6539/00/0604-0740 $ 17.50+.50/0 *Chem. Eur. J.* **2000**, *6*, No. 4

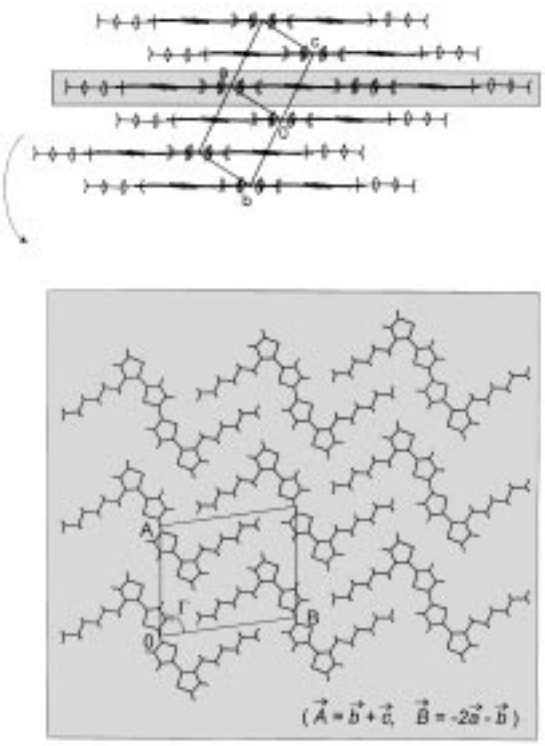

Figure 9. Molecular packing of **2** viewed from the [011] direction (top). View from the direction normal to the (1 −22) plane (bottom). Only the molecules on the same plane are drawn.

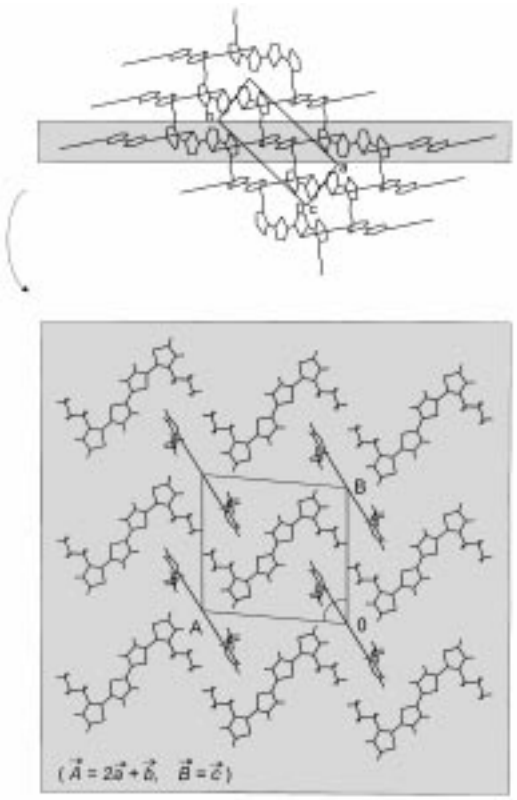

Figure 10. Molecular packing of **3** viewed from the [001] direction (top). Hydrogen atoms are omitted for simplicity. View from the direction normal to the (120) plane (bottom). Only the molecules on the same plane are drawn. In both figures, one of the independent quaterthiophene molecules has two thiophene rings that are completely parallel to the view direction. These rings are therefore seen just as solid lines.

plane of the bulk crystal has a good coincidence with the two-dimensional molecular arrangement in the adsorbed monolayer at the solution–HOPG interface and exhibits nearly identical "lattice constants" (Figure 3, Table 1).

In contrast to quaterthiophene **1** and **2**, crystals of propyl derivative **3** exhibit a different packing of the molecules (Figure 10). The longer molecular axis of the quaterthiophene backbone is oblique with respect to the neighboring molecule, and the molecular planes are tilted with each other. The packing motif resembles that observed for 3,3‴-dimethoxyquaterthiophene.[10k] In comparison with compounds **1** and **2**, the difference of the crystal structures arises from the alkyl side chains: propyl chains are too short to maintain the hydrophobic interactions between themselves. Therefore, a lamellae structure observed for **1** and **2** can not be achieved. Despite of the complicated molecular packing, two-dimensional "sheets" can also be defined in the case of derivative **3** (Figure 10, top). The heteroaromatic rings of every second oligothiophene are nearly perpendicular with respect to the "sheet", and the propyl side chains stick into the neighboring layers. The arrangement of the molecules in this "cross-section" of the crystal (Figure 10, bottom) nevertheless clearly resembles that observed in the STM image of the dip-coated film of quaterthiophene **3** on the HOPG surface. This suggests that the dip-coated two-dimensional film on HOPG exhibits the same molecular arrangement comprising similar "lattice constants" as the "cross-section" of the three-dimensional bulk crystal (Figure 4, Table 1).

These results show that the two-dimensional arrangement of compounds observed at the HOPG surface with STM correspond well with at least one plane or "cross-section" in the three-dimensional structure of the same materials, although there is an additional influence of the substrate on the ordering behavior, because the direction of the rows is not random but limited (see Figure 1).

Discussion

The results described above provide a good example for the discussion of the correlation of the two-dimensional and three-dimensional molecular arrangements. In the case of compounds **1** and **2**, the "lattice constants" of the two-dimensional crystalline adsorbate at the HOPG interface and those in one of the "cross-sections" of the bulk crystal are almost identical (Table 1). This finding suggests that the packing of the molecules in these two different states is essentially the same. The molecular arrangement of **1** in the (103) plane of the bulk crystal is superimposed on the STM images of the monolayer of **1** and the underlying HOPG lattice (Figure 11). Assuming that the conformation of the molecules in the monolayer on HOPG is similar to that in the bulk crystal, that is, if the long axes of the alkyl chains are almost perpendicular to the quaterthiophene backbone, then the alkyl chains are parallel to the direction of the main crystallographic axis of HOPG. If we also take into consid-

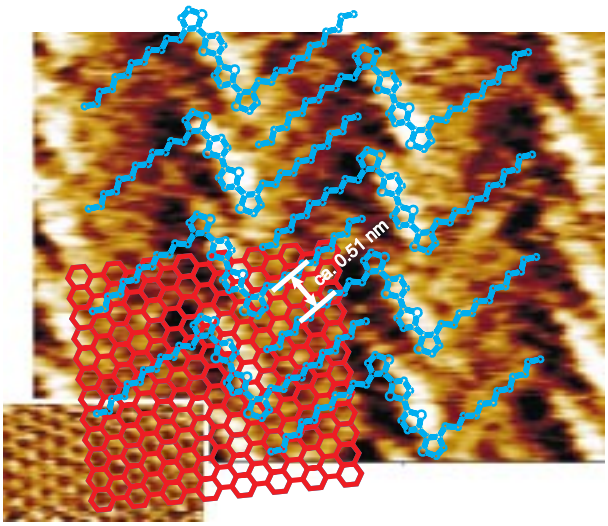

Figure 11. Scheme of the molecular arrangement in the absorbed monolayer of quaterthiophene **1** and the underlying HOPG. Note that the lateral positioning of the STM pictures of the absorbed monolayer and HOPG is meaningless due to drift during the measurement. Furthermore, the lattice of the adsorbed monolayer is not commensurate with that of HOPG (see text). Only the size of each lattice and the relative orientation should be regarded.

eration the result that there are only six different possibilities for how the rows in the domains are oriented (see Figure 1), then this result suggests that the alkyl side chains of the molecules are epitaxially adsorbed on HOPG. This effect is evidently the driving force for the attraction of molecules to the surface, as was also found for other compounds.[12–15] The existence of twice as many directions of rows (six) as numbers of equivalent crystallographic axes of HOPG (three) is simply explained by the existence of two different directions of rows of oligothiophene backbone for the same orientation of alkyl chains (Figure 12). In other words, a pair of "enantiomorphic" domains,[17b] for each direction of the alkyl chains exists.

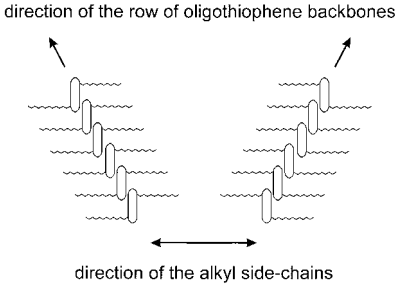

Figure 12. Two possible "enantiomorphic" stacking features of oligothiophenes including the same direction of the alkyl side chains.

The determination of the distance between two adjacent alkyl side chains (0.51 nm) reveals that there is no absolute match of the carbons in the chain with the underlying substrate in this direction. Therefore, not all alkyl chains take any particular site of the substrate. Evidently, besides the molecule–substrate interactions, intermolecular forces also play an important role in the formation and stabilization of the self-assembled monolayers.

The propyl chains in compound **3** are too short to form a stable monolayer at the liquid–solid interface. This finding also proves that sufficiently strong interactions between alkyl side chains and HOPG are necessary to form a monolayer at the solution–graphite interface. In accordance with derivatives **1** and **2**, the two-dimensional molecular arrangement of **3** on HOPG resembles most remarkably the molecular packing in one of the "cross-sections" or "sheets" in the three-dimensional bulk crystal. However, in this case, the discussion is slightly ambiguous. It is not clear from the STM images whether the thiophene rings of every second molecule are tilted with respect to the plane, as can be seen in the bulk crystal, or whether the thiophene rings of all molecules in the adsorbed layer lie flat on the surface. For these two cases, the "lattice constants" of the two-dimensional layer would not dramatically change and the difference could be within the experimental error of the STM measurements.

For all three compounds the molecular order in a two-dimensional layer on a substrate and in a layer of the three-dimensional crystal is nearly the same. Unless the molecule–substrate interactions are too large, one could thus predict the molecular packing in bulk crystals from the order in two-dimensional layers of the same compound. This also shows that a crystalline domain, when forced to grow two-dimensionally, tends to grow in the directions of a representative "sheet" in a crystal due to the stronger intermolecular interactions in these directions.

The above results also demonstrate the effect of alkyl side chains on the molecular organization. The dodecyl chains of quaterthiophene **1** stack and interlock with themselves. In contrast, due to the shorter alkyl side chains, the molecular arrangement of propyl derivative **3** is totally different from that of derivative **1**, both in the dip-coated film on the surface and in the three-dimensional crystal. This means that the propyl chains of compound **3** are too short to maintain the packing with neighboring chains. Hexyl chains in compound **2** are sufficiently long to provide hydrophobic alkyl–alkyl interactions, and packing as for compound **1** is observed; however, the length approaches the shortest limit below which the molecular packing turns into another type as was observed for compound **3**. The anomalous low melting point of quaterthiophene **2** (27–28 °C) is thus understandable: the hydrophobic interactions due to hexyl chains are too weak in order to maintain the crystal lattice up to higher temperatures. The results described above are also informative for the understanding of the molecular packing of alkylated polythiophenes. In this respect, it was reported that one of the *d* spacings in the polycrystalline part of poly(3-alkylthiophene)s, obtained with X-ray powder diffraction measurements, linearly increases with the length of alkyl side chains, except for the case of the methyl derivative.[7a] In accordance with our results, the authors suggest that polymers with shorter alkyl side chains exhibit a different molecular packing in comparison with those with longer alkyl side chains. Therefore, the length of the alkyl side chains strongly affects the molecular packing, and consequently influences the physical properties of the solid-state material.

0947-6539/00/0604-0742 $ 17.50+.50/0 *Chem. Eur. J.* **2000**, *6*, No. 4

Conclusion

We have demonstrated that the combination of STM investigations on two-dimensional monolayers at a substrate interface and X-ray single-crystal analyses enables us to gain a better understanding on the self-assembling properties of oligothiophenes. The quaterthiophenes **1** and **2** which have longer alkyl side chains attached to β-positions exhibit a molecular order in which the alkyl chains are packed with one another, both in the two-dimensional layers at the surface and in the three-dimensional bulk crystals. Derivative **3** which bears the shorter propyl chains has a completely different tendency to order due to the lack of sufficiently strong intermolecular interactions of the alkyl chains. In all three cases, the two-dimensional arrangement of the adsorbates observed at the HOPG surface most notably coincides well with the molecular order in one layer of the three-dimensional crystal. This clearly indicates that information on the self-assembling properties of materials obtained from STM investigations are extremely valuable in order to understand the ordering in three-dimensional solids. If the molecule–substrate interactions are not too dominating, STM provides an excellent additional way to quickly get information about the molecular packing in the solid state when it is impossible to perform the X-ray single-crystal analyses.

Experimental Section

General: Solvents and reagents were purified and dried by usual methods prior to use. Thin-layer chromatography (TLC) was carried out on plastic plates (Polygram SIL and Polygram Alox from Macherey and Nagel). Developed plates were dried and scrutinized under a UV lamp. Preparative column chromatography was performed on glass columns of different sizes packed with Kieselgel 60 (20–200 μm, Merck). Melting points were determined with Electrothermal 9100 melting point apparatus and are uncorrected. ^{1}H NMR spectra were recorded on Bruker DMX600 (600 MHz), AMX500 (500 MHz), and ACF250 (250 MHz) spectrometers (with deuterated solvent as lock-in and tetramethylsilane as internal reference). ^{13}C NMR spectra were recorded on Bruker DMX600 (151 MHz), AMX500 (126 MHz), and ACF250 (63 MHz) spectrometers. Elemental analyses were performed on a Carlo Erba Instrumentatione Elementar Analyser 1106.

Scanning tunneling microscopy: Measurements were carried out with a low-current scanning tunneling microscope (Digital Instruments) equipped with a Nanoscope IIIa controller (Digital Instruments) at room temperature. Mechanically cut Pt/It tips were used. For the measurement at the solution–substrate interface, a nearly saturated solution of the quaterthiophene in 1,2,4-trichlorobenzene was applied onto a freshly cleaved (001) face of HOPG. For the measurement of dip-coated films, the substrate was dipped into a diluted solution of the quaterthiophene in chloroform, withdrawn, and dried in air. The images are shown as obtained (i.e. distortion of the images due to drift is uncorrected), while the velocity of drift at each measurement is considered in the calculation of "two-dimensional lattice constants". Measurement conditions are given in the corresponding figure captions.

X-ray crystal structure analysis: Single crystals were obtained by slow evaporation of solutions of **1** in *n*-hexane, of **2** in a mixture of *n*-hexane and ethanol, and of **3** in petroleum ether. The crystallization of oligomer **2** was performed at 4 °C. Diffraction data were collected on a STOE-IPDS image plate diffractometer ($Mo_{K\alpha}$ radiation, graphite monochromator) in the φ rotation scan mode. The measured intensities were corrected for Lorentz and polarization effects. The structure determination was done with direct methods by using XMY[22] and refinements with full-matrix least-squares on F^2 with SHELXL-97.[23] The positions of hydrogen atoms were calculated and refined isotropically. The graphics were performed with ORTEP3[24] and PLATON.[25] Crystal data and refinement parameters are given in Tables 2 and 3. Crystallographic data (excluding structure factors) for the structures reported in this paper have been deposited with the Cambridge Crystallographic Data Centre as supplementary publication no. CCDC-118941, CCDC-118942, and CCDC 118943. Copies of the data can be obtained free of charge on application to CCDC, 12 Union Road, Cambridge CB2 1EZ, UK (Fax: (+44) 1223 336-033; e-mail: deposit@ccdc.cam.ac.uk).

Starting materials: The starting materials were prepared according to literature procedures: 3-dodecyl-2-bromothiophene[26] (b.p. 122–125 °C/10^{-3} mbar, yield 71%), 3-hexyl-2-bromothiophene[27] (b.p. 137 °C/18 mbar, yield 70%), 3-propyl-2-bromothiophene[28] (b.p. 91 °C/18 mbar, yield 78%), 5,5′-dibromo-2,2′-bithiophene[29] (m.p. 146 °C, yield 70%).

3,3‴-Didodecyl-2,2′:5′,2″:5″,2‴-quaterthiophene (1): 2-Bromo-3-dodecylthiophene (31.8 g, 96.1 mmol) in anhydrous diethyl ether (25 mL) was added under inert atmosphere to magnesium turnings (2.34 g, 96.3 mmol) in diethyl ether (5 mL). The reaction mixture was then heated under reflux for 1 h. This Grignard solution was subsequently transferred through a cannula to a second apparatus and added slowly to a boiling solution of 5,5′-dibromo-2,2′-bithiophene (12.5 g, 38.4 mmol) and [Ni(dppp)Cl_2] (88 mg, 0.16mmol) in diethyl ether (300 mL) over 1 h. The reaction mixture was heated under reflux for 5 d and afterwards hydrolyzed with cold HCl (1N) followed by extraction with diethyl ether. The combined organic phases were washed with water neutralized with saturated $NaHCO_3$ and dried. After removal of the solvent in vacuo the residue was purified by two chromatographic steps on columns of silica gel of different grain size at normal (A60; 32–63 μm) and increased pressure (LiChroSpher; 15–25 μm). Finally, the product was recrystallized from *n*-pentane to yield 18.45 g (72%) of a yellow solid. M.p. 59–60 °C; ^{1}H NMR (250 MHz, $CDCl_3$): $\delta = 7.15$ (d, $^3J_{(H5,4)} = 5.2$ Hz, 2H; H5,5‴), 7.10 (d, $^3J_{(H4,3)} = 3.8$ Hz, 2H; H4′,3″), 7.00 (d, $^3J_{(H3,4)} = 3.8$ Hz, 2H; H3′,4″), 6.92 (d, $^3J_{(H4,5)} = 5.2$ Hz, 2H; H4,4‴), 2.77 (t, $J_{(H\alpha,\beta)} = 7.8$ Hz, 4H; α-CH_2), 1.64 (m, 4H; β-CH_2), 1.24 (m, 36H; CH_2), 0.87 (t, 6H; CH_3); ^{13}C NMR (63 MHz, $CDCl_3$): $\delta = 139.9$, 136.8, 135.3, 130.3, 130.1, 126.5, 123.8, 31.9, 30.7, 29.7, 29.6, 29.5, 29.4, 29.3, 22.7, 14.1; $C_{40}H_{58}S_4$ (667.14): calcd C 72.01, H 8.76, S 19.22; found C 72.12, H 8.81, S 18.99.

3,3‴-Dihexyl-2,2′:5′,2″:5″,2‴-quaterthiophene (2): A Grignard solution was prepared from 2-bromo-3-hexylthiophene (2.67 g, 10 mmol) in anhydrous diethyl ether (10 mL) and magnesium turnings (0.24 g, 10 mmol) in diethyl ether (1 mL) according to the preceding procedure. The solution was heated under reflux for 4 h, then transfered to a second apparatus and added slowly to a solution of 5,5′-dibromo-2,2′-bithiophene (1.43 g, 4.4 mmol) and [Ni(dppp)Cl_2] (20 mg, 0.04 mmol) in diethyl ether (7 mL) at room temperature. The reaction mixture was heated under reflux for 19 h, quenched with cold water and HCl (1N), and extracted with several portions of ether. Washing to neutrality, drying of the combined organic phases, and removal of the solvent in vacuo afforded a crude product, which was purified on a column of silica gel with petroleum ether (b.p. 50–60 °C) and recrystallized from petroleum ether (b.p. 30–40 °C). Yield: 0.88 g (44%); m.p. 27–28 °C; ^{1}H NMR (200 MHz, $CDCl_3$): $\delta = 7.09$ (d, $^3J_{(H5,4)} = 5.4$ Hz, 2H; H5,5‴), 7.04 (d, $^3J_{(H4',3')} = 3.4$ Hz, 2H; H4′,3″), 6.94 (d, $^3J_{(H3',4')} = 3.5$ Hz, 2H; H3′,4″), 6.86 (d, $^3J_{(H4,5)} = 5.4$ Hz, 2H; H4,4‴), 2.70 (t, $J_{(H\alpha,\beta)} = 7.4$ Hz, 4H; α-CH_2), 1.57 (m, 4H; β-CH_2), 1.25 (m, 12H; CH_2), 0.81 (t, 6H; CH_3); $C_{28}H_{34}S_4$ (498.84): calcd C 67.42, H 6.87, S 25.71; found C 67.36, H 6.85, S 25.85.

3,3‴-Dipropyl-2,2′:5′,2″:5″,2‴-quaterthiophene (3): From a solution of 2-bromo-3-propylthiophene (5.13 g, 25 mmol) in anhydrous diethyl ether (17 mL) and magnesium turnings (0.61 g, 25 mmol) in diethyl ether (2 mL), the Grignard reagent was generated according the above procedures. This solution was heated under reflux for 1.5 h and transferred afterwards to a second apparatus, which was charged with a suspension of 5,5′-dibromo-2,2′-bithiophene (3.24 g, 10 mmol) and [Ni(dppp)Cl_2] (27 mg, 0.05 mmol) in diethyl ether (15 mL). The Grignard solution was added at room temperature and the reaction mixture heated under reflux for 24 h. A second portion of [Ni(dppp)Cl_2] (27 mg, 0.05 mmol) was added after 5 h of heating under reflux. Work up with cold water and HCl (1N) as described above and extraction with ether left a red solid after evaporation of the solvent; this solid was filtered on a short silica gel column with petroleum ether (b.p. 50–60 °C). The product was recrystallized from the same solvent

to afford 3.65 g (88 %) of analytically pure compund. M.p. 63 °C; ^{1}H NMR (200 MHz, $CDCl_3$): $\delta = 7.10$ (d, $^3J_{(H5,4)} = 5$ Hz, 2H; H5,5‴), 7.04 (d, $^3J_{(H4',3')} = 3.4$ Hz, 2H; H4′,3″), 6.94 (d, $^3J_{(H3',4')} = 3.4$ Hz, 2H; H3′,4″), 6.86 (d, $^3J_{(H4,5)} = 5$ Hz, 2H; H4,4‴), 2.70 (t, $^3J_{(H\alpha,\beta)} = 7.7$ Hz, 4H; α-CH_2), 1.62 (m, 4H; β-CH_2), 0.93 (t, $^3J = 7.4$ Hz, 6H; CH_3); $C_{22}H_{22}S_4$ (414.68): calcd C 63.72, H 5.35, S 30.93; found C 63.62, H 5.27, S 31.22.

Acknowledgements

Acknowledgments: We would like to thank the Alexander von Humboldt foundation for a research fellowship for R.A. This work was financially supported by the Deutsche Forschungsgemeinschaft (SFB 239) and the EU (Frequent-Esprit 24793). We also acknowledge Prof. Dr. M. Möller, Dr. A. E. Semenow, and Dr. J. P. Spatz (Abteilung Organische Chemie III, Universität Ulm) for initially providing their STM equipment and helpful suggestions.

[1] *Handbook of Oligo- and Polythiophenes* (Ed.: D. Fichou), Wiley-VCH, Weinheim, **1998**.
[2] P. Bäuerle, in *Electronic Materials: The Oligomer Approach* (Eds.: K. Müllen, G. Wegner), Wiley-VCH, Weinheim, **1998**, chapter 2.
[3] *Handbook of Conducting Polymers* (Eds.: T. A. Skotheim, R. L. Elsenbaumer, J. R. Reynolds), 2nd ed., Marcel Dekker, New York, **1998**.
[4] M. G. Harrison, R. H. Friend, in *Electronic Materials: The Oligomer Approach* (Eds.: K. Müllen, G. Wegner) Wiley-VCH, Weinheim, **1998**, chapter 10.
[5] F. Garnier, in *Electronic Materials: The Oligomer Approach* (Eds.: K. Müllen, G. Wegner), Wiley-VCH, Weinheim, **1998**, chapter 11.
[6] D. Fichou, C. Ziegler, in *Handbook of Oligo- and Polythiophenes* (Ed.: D. Fichou), Wiley-VCH, Weinheim, **1998**, chapter 4.
[7] a) F. Garnier, G. Tourillon, J. Y. Barraud, H. Dexpert, *J. Mater. Sci*. **1985**, *20*, 2687 – 2694; b) K. Tashiro, K. Ono, Y. Minagawa, M. Kobayashi, T. Kawai, K. Yoshino, *J. Polym. Sci. Part B: Polym. Phys.* **1991**, *129*, 1223 – 1233; c) T. J. Prosa, M. J. Winokur, J. Moulton, P. Smith, A. J. Heeger, *Macromolecules* **1992**, *25*, 4364 – 4372; d) T. Yamamoto, D. Komarudin, M. Arai, B.-L. Lee, H. Suganuma, N. Asakawa, Y. Inoue, K. Kubota, S. Sasaki, T. Fukuda, H. Matsuda, *J. Am. Chem. Soc.* **1998**, *120*, 2047 – 2058.
[8] R. D. McCullough, *Adv. Mater.* **1998**, *10*, 93 – 116.
[9] a) R. D. McCullough, S. Tristram-Nagle, S. P. Williams, R. D. Lowe, M. Jayaraman, *J. Am. Chem. Soc*. **1993**, *115*, 4910 – 4911; b) T.-A. Chen, X. Wu, R. D. Rieke, *J. Am. Chem. Soc*. **1995**, *117*, 233 – 244; c) S. V. Meille, V. Romita, T. Caronna, A. J. Lovinger, M. Catellani, L. Belobrzeckaja, *Macromolecules* **1997**, *30*, 7898 – 7905; d) T. Kaniowski, W. Luzny, S. Niziol, J. Sanetra, M. Trznadel, *Synth. Met*. **1998**, *92*, 7 – 12.
[10] a) *α-2T*: M. Pelletier, F. Brisse, *Acta Crystallogr. Sect. C* **1994**, *50*, 1942 – 1945; b) *α-3T*: F. van Bolhuis, H. Wynberg, E. E. Havinga, E. W. Meijer, E. G. J. Starring, *Synth. Met.* **1989**, *30*, 381 – 389; c) *α-4T*: T. Siegrist, C. Kloc, R. A. Laudise, H. E. Katz, R. C. Haddon, *Adv. Mater.* **1998**, *10*, 379 – 382; L. Antolini, G. Horowitz, F. Kouki, F. Garnier, *Adv. Mater.* **1998**, *10*, 382 – 385; d) *α-6T*: G. Horowitz, B. Bachet, A. Yassar, P. Lang, F. Demanze, J. L. Fave, F. Garnier, *Chem. Mater.* **1995**, *7*, 1337 – 1341; e) *α-8T*: D. Fichou, B. Bachet, F. Demanze, I. Billy, G. Horowitz, F. Garnier, *Adv. Mater*. **1996**, *8*, 500 – 504. f) *Trimethyl-α-3T*: G. Barbarella, M. Zambianchi, A. Bongini, L. Antolini, *Adv. Mater*. **1994**, *6*, 561 – 564; g) *Subst.-α-3T*: P. A. Chaloner, S. R. Gunatunga, P. B. Hitchcock, *J. Chem. Soc. Perkin Trans. 2* **1997**, 1597 – 1604; h) *Dimethyl-α-4T*: S. Hotta, J. Waragai, *J. Mater. Chem*. **1991**, *1*, 835 – 842; i) *Tetramethyl-α-4T*: G. Barbarella, M. Zambianchi, A. Bongini, L. Antolini, *Adv. Mater*. **1992**, *4*, 282 – 285; j) *Dimethyl-α-4T, Tetramethyl-α-4T*: G. Barbarella, M. Zambianchi, A. Bongini, L. Antolini, *Adv. Mater*. **1993**, *5*, 834 – 838; k) *Dimethoxy-α-4T*: L. L. Miller, Y. Yu, *J. Org. Chem.* **1995**, *60*, 6813 – 6819; l) *Tetrathiomethyl-α-4T*: G. Barbarella, M. Zambianchi, M. del Fresno, I. Marimon, L. Antolini, A. Bongini, *Adv. Mater*. **1997**, *9*, 484 – 487; m) *Dibutyl-α-5T, tetrabutyl-α-6T*: J.-H. Liao, M. Benz, E. LeGoff, M. G. Kanatzidis, *Adv. Mater*. **1994**, *6*, 135 – 138; n) *Dibutyl-α-6T*: J. K. Herrema, J. Wildeman, F. van Bolhuis, G. Hadziioannou, *Synth. Met.* **1993**, *60*, 239 – 248; o) *Dihexyl-α-6T*: T. Sato, M. Fujitsuka, M. Shiro, K. Tanaka, *Synth. Met.* **1998**, *95*, 143 – 148; p) *Bis(triisopropylsilyl)-α-6T*: A. Yassar, F. Garnier, F. Deloffre, G. Horowitz, L. Ricard, *Adv. Mater*. **1994**, *6*, 660 – 663; q) *Dicyano-α-nT (n = 3 – 6)*: T. M. Barclay, A. W. Cordes, C. D. MacKinnon, R. T. Oakley, R. W. Reed, *Chem. Mater*. **1997**, *9*, 981 – 990.
[11] a) M. Hara, Y. Iwakabe, K. Tochigi, H. Sasabe, A. F. Garito, A. Yamada, *Nature* **1990**, *344*, 228 – 230; b) Y. Iwakabe, M. Hara, K. Kondo, K. Tochigi, A. Mukoh, A. Yamada, A. F. Garito, H. Sasabe, *Jpn. J. Appl. Phys.* **1991**, *30*, 2542 – 2546; c) D. P. E. Smith, J. K. H. Hörber, G. Binnig, H. Nejoh, *Nature* **1990**, *344*, 641 – 644; d) D. P. E. Smith, W. M. Heckl, *Nature* **1990**, *346*, 616 – 617.
[12] a) G. C. McGonigal, R. H. Bernhardt, D. J. Thomson, *Appl. Phys. Lett.* **1990**, *57*, 28 – 30; b) J. P. Rabe, S. Buchholz, *Science* **1991**, *253*, 424 – 427; c) G. Watel, F. Thibaudau, J. Cousty, *Surf. Sci. Lett.* **1993**, *281*, L297-L302.
[13] A. Wawkuschewski, H.-J. Cantow, S. N. Magonov, M. Möller, W. Liang, M.-H. Whangbo, *Adv. Mat.* **1993**, *5*, 821 – 826.
[14] M. Hibino, A. Sumi, I. Hatta, *Jpn. J. Appl. Phys.* **1995**, *34*, 610 – 614.
[15] a) A. Stabel, R. Heinz, F. C. De Schryver, J. P. Rabe, *J. Phys. Chem.* **1995**, *99*, 505 – 507; b) A. Stabel, P. Herwig, K. Müllen, J. P. Rabe, *Angew. Chem.* **1995**, *107*, 1768 – 1770; *Angew. Chem. Int. Ed. Engl.* **1995**, *34*, 1609 – 1611; c) P. C. M. Grim, S. De Feyter, A. Gesquiere, P. Vanoppen, M. Rücker, S. Valiyaveettil, G. Moessner, K. Müllen, F. C. De Schryver, *Angew. Chem.* **1997**, *109*, 2713 – 2715; *Angew. Chem. Int. Ed. Engl.* **1997**, *36*, 2601 – 2603; d) S. De Feyter, P. C. M. Grim, M. Rücker, P. Vanoppen, C. Meiners, M. Sieffert, S. Valiyaveettil, K. Müllen, F. C. De Schryver, *Angew. Chem.* **1998**, *100*, 1281 – 1284; *Angew. Chem. Int. Ed.* **1998**, *37*, 1223 – 1226; e) K. Eichhorst-Gerner, A. Stabel, G. Moessner, D. Declerq, S. Valiyaveettil, V. Enkelmann, K. Müllen, J. P. Rabe, *Angew. Chem.* **1996**, *108*, 1599 – 1602; *Angew. Chem. Int. Ed. Engl.* **1996**, *35*, 1492 – 1495; f) D. M. Cyr, B. Venkataraman, G. W. Flynn, *Chem. Mater.* **1996**, *8*, 1600 – 1615; g) T.-L. Liu, J. P. Parakka, M. P. Cava, Y.-T. Kim, *Synth. Met.* **1995**, *71*, 1989 – 1992; h) F. Stevens, D. J. Dyer, D. M. Walba, *Angew. Chem.* **1996**, *108*, 955 – 957; *Angew. Chem. Int. Ed. Engl.* **1996**, *35*, 900 – 901.
[16] S. Chang, in *Scanning Tunneling Microscopy I* (Eds.: H.-J. Güntherodt, R. Wiesendanger), 2nd ed., Springer, Berlin **1994**, chapter 7.
[17] a) W. M. Heckl, D. P. E. Smith, G. Binnig, H. Klagges, T. W. Hänsch, J. Maddocks, *Proc. Natl. Acad. Sci. USA* **1991**, *88*, 8003 – 8005; b) S. J. Sowerby, W. M. Heckl, G. B. Petersen, *J. Mol. Evol.* **1996**, *43*, 419 – 424.
[18] a) A. Stabel, J. P. Rabe, *Synth. Met.* **1994**, *67*, 47 – 53; b) P. Bäuerle, T. Fischer, B. Bidlingmeier, A. Stabel, J. P. Rabe, *Angew. Chem.* **1995**, *107*, 335 – 339; *Angew. Chem. Int. Ed. Engl.* **1995**, *34*, 303 – 307; c) H. Müller, J. Petersen, R. Strohmaier, B. Gompf, W. Eisenmenger, M. S. Vollmer, F. Effenberger, *Adv. Mater.* **1996**, *8*, 733 – 737; d) T. Kirschbaum, R. Azumi, E. Mena-Osteritz, P. Bäuerle, *New J. Chem.* **1999**, *23*, 241 – 251; e) M. S. Vollmer, F. Effenberger, R. Stecher, B. Gompf, W. Eisenmenger, *Chem. Eur. J.* **1999**, *5*, 96 – 101; f) R. Azumi, G. Götz, P. Bäuerle, *Synth. Met.* **1999**, *101*, 569 – 572.
[19] E. Mena-Osteritz, P. Bäuerle, unpublished results. This finding corresponds to an "end-effect" of the conjugation in the terminal thiophene rings.
[20] a) D. W. J. Cruickshank, *Acta Crystallogr.* **1956**, *9*, 757 – 758; b) D. W. J. Cruickshank, *Acta Crystallogr.* **1956**, *14*, 896 – 897; c) L. N. Becka, D. W. J. Cruickshank, *Acta Crystallogr.* **1956**, *14*, 1092.
[21] A. Bondi, *J. Phys. Chem.* **1964**, *68*, 441.
[22] T. Debaerdemaeker, *Z. Krist.* **1993**, *206*, 173 – 182.
[23] G. M. Sheldrick, *SHELXL93*, University of Göttingen, **1993**.
[24] L. J. Farrugia, *J. Appl. Crystallogr.* **1997**, *30*, 565.
[25] A. L. Spek, *Acta Crystallogr. Sect. A* **1990**, *46*, C34.
[26] P. Bäuerle, F. Pfau, H. Schlupp, F. Würthner, K.-U. Gaudl, M. B. Caro, P. Fischer, *J. Chem. Soc. Perkin Trans 2* **1993**, 489 – 494.
[27] H. Higuchi, T. Nakayama, H. Koyama, J. Ojima, T. Wada, H. Sasabe, *Bull. Chem. Soc. Jpn.* **1995**, *68*, 2363 – 2377.
[28] G. Consiglio, S. Gronowitz, A.-B. Hörnfeldt, B. Mattesson, R. Notto, D. Spinelli, *Chem. Scr.* **1977**, *11*, 175 – 179.
[29] P. Bäuerle, F. Würthner, G. Götz, F. Effenberger, *Synthesis* **1993**, 1099 – 1103.

Received: April 29, 1999
Revised Version: July 2, 1999 [F1755]

  0947-6539/00/0604-0744 $ 17.50+.50/0